

Neutron cross sections in stellar nucleosynthesis: Study of the key isotope ^{25}Mg

F. MINGRONE

INFN, Sezione di Bologna and Università di Bologna - Bologna, Italy

ricevuto il 31 gennaio 2014; approvato il 3 Giugno 2014

Summary. — In this document the important role of ^{25}Mg within nucleosynthesis processes is studied. In fact the initial conditions of s-process in massive and AGB stars depend on neutron-induced reactions on ^{25}Mg , being this isotope involved both in neutron production and as a neutron poison. Because of the importance of ^{25}Mg , very accurate and precise measurements of its capture cross section, at the n_TOF CERN facility, and of its total cross section, at the EC-JRC-IRMM facility in Belgium, were performed. The aims of these measurements are both to weight the contribution of ^{25}Mg as a neutron poison and to give constraints for the reaction rate of one of the main neutron sources for the s-process.

PACS 26.20.Kn – Hydrostatic stellar nucleosynthesis: s-process.

PACS 28.20.Np – Nuclear engineering and nuclear power studies: Neutron capture γ -rays.

PACS 25.40.Lw – Nucleon-induced reactions: Radiative capture.

PACS 29.30.Hs – Spectrometers and spectroscopy techniques: Neutron spectroscopy.

1. – Introduction

Elements heavier than iron are produced in stellar environment through the balance of neutron capture and β -decay processes. About a half of these elements appears throughout the nucleosynthesis chain of the so-called s-process, *i.e.* the slow neutron capture process [1]. The main astrophysical site for the s-process is identified in stars with low masses, between one and three solar masses, during their asymptotic giant branch (AGB) phase, where they experience a series of He-shell flashes called thermal pulses. In this *main* s-process most of the isotopes from strontium to lead and bismuth are synthesised. There is a second component of the s-process, called *weak*, which synthesises most of the isotopes between iron and strontium and occurs in nuclear burning phases of massive stars (helium-burning core and subsequent carbon-burning shell).

Although most of the astrophysical sites of the stellar nucleosynthesis and the nuclear processes involved have been identified, important physical and nuclear details are still

largely unexplained, thus hindering a comprehensive understanding of the origin of the elements. In this view, an accurate knowledge of the nuclear reaction rates at stellar energy is fundamental to constrain theoretical predictions of stellar models.

The (α, n) reaction on ^{22}Ne is the the major astrophysical neutron source of the s-process in massive stars and in intermediate AGB stars, while it is partially activated in low mass AGBs. Despite lots of attempts (see [2] and reference therein), direct measurements at the energy range of astrophysical sites (*i.e.* keV energy region) are extremely difficult, mostly because of the extremely low cross section of the reaction at these energies and of cosmic-ray-induced background. Data present in the literature are therefore not accurate or even lacking, with the consequence that the $^{22}\text{Ne}(\alpha, n)^{25}\text{Mg}$ reaction rate is very uncertain. This reaction rate at s-process temperature depends on the levels structure of the compound nucleus ^{26}Mg above the α threshold ($Q = 10.615$ MeV) and nearby the neutron threshold ($S_n = 11.093$ MeV). The properties of these states are poorly known, nevertheless information on their spin-parity J^π can be obtained studying a different reaction, *i.e.* $^{25}\text{Mg}(n, \gamma)^{26}\text{Mg}$, and selecting only those states which can be populated by $^{22}\text{Ne} + \alpha$ reaction. For both ^{22}Ne and α particle, in fact, $J^\pi = 0^+$, and so only natural parity states ($0^+, 1^-, 2^+, \dots$) can participate in the $^{22}\text{Ne}(\alpha, n)^{25}\text{Mg}$ reaction, which correspond to a subset of ^{26}Mg states populated in the $^{25}\text{Mg}(n, \gamma)^{26}\text{Mg}$ reaction. Therefore, it is crucial to have an extremely precise assignation of the spin-parity numbers to each state studied in $^{25}\text{Mg} + n$ reaction.

Moreover, ^{25}Mg is considered one of the main neutron poisons at the onset of s-process: neutron capture on ^{25}Mg , in fact, affects the efficiency for the production of heavy element, starting from neutron capture on ^{56}Fe , which is the basic s-process seed for the production of heavy isotopes. For this reason an accurate knowledge of the $^{25}\text{Mg}(n, \gamma)^{26}\text{Mg}$ reaction cross section is required to estimate the contribution of ^{25}Mg as a neutron poison.

As pointed out, the initial conditions of the s-process nucleosynthesis chain strongly depend on $n+^{25}\text{Mg}$ reactions. Because of its relevance, a measurement of the $^{25}\text{Mg}(n, \gamma)$ cross section was performed in 2003 at the CERN n_TOF facility [3]. Unfortunately, the sample analysed was not well suited for the measurement, resulting in the introduction of different sources of uncertainties. Because of the need of precise and accurate data, a second measurement was proposed [4] and performed at n_TOF in 2012 with an upgraded experimental set up. In addition, at the EC-JRC-IRMM facility GELINA, in Belgium, the total cross section on ^{25}Mg was proposed [4] and measured.

The experimental technique will be described, and the results of these new measurements will be shown together with the comparison with previous data.

2. – Capture experiment

2.1. Experimental method. – The measurement of $^{25}\text{Mg}(n, \gamma)$ cross section was performed at the neutron time-of-flight facility of CERN, n_TOF, in June 2012. At this facility neutrons are generated in spallation reactions by a pulsed 20 GeV/c proton beam impinging on a lead block (see fig. 1), surrounded by 4 cm of water plus 1 cm of borated water which serves as a coolant and as a moderator of the originally fast neutron spectrum [5]. The resulting white neutron beam ranges from thermal energies to 1 GeV. The neutrons travel through an evacuated beam line to the experimental area at a distance of about 185 m from the spallation target, where the sample and the detection systems are placed. During the entire measurement the flux at the sample position is kept under control by a thin ^6Li foil that is placed in beam and viewed by a silicon detector [6].

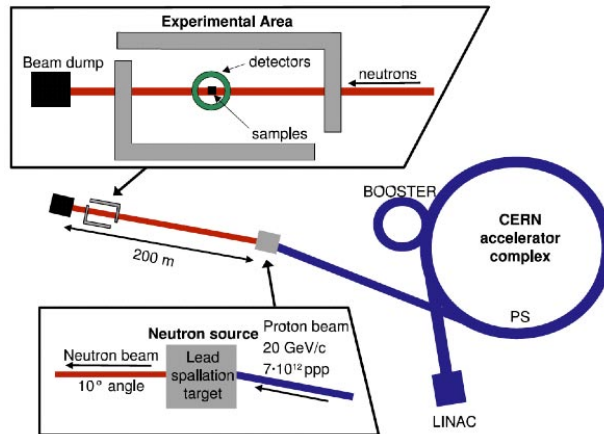


Fig. 1. – Layout of the n_TOF facility within the CERN accelerator complex.

The very long flight path, together with an extremely high instantaneous neutron flux at the experimental area and a low repetition rate (1 pulse is sent from the PS each 2.4 s) allow to perform very accurate (n, γ) cross section measurements in an energy range from thermal to about 1 MeV.

The data acquisition system is based on Flash Analogue-to-Digital Converters (*flash-ADC*) used for sampling and recording the waveform of the detector signals. After zero suppression, the data are sent to CERN data storage facility CASTOR, while an on-line analysis with dedicated pulse shape analysis routines for each detector is performed for monitoring the quality of the data.

The γ -rays following the radiative neutron capture on ^{25}Mg were measured with a low-solid-angle detection system in order to apply the total energy detection method, which requires a very low single- γ efficiency. Two deuterated benzene scintillators were used, placed head to head at 90° with respect to the beam, 9 mm away from the sample (see fig. 2): one commercial Bicron BC-537 and one custom made (developed at the Forschungszentrum Karlsruhe - FZK) [7]. Both the detectors and the geometry are optimised to have a very low sensitivity to γ -rays induced by scattered neutrons. To express the light output of the C_6D_6 detectors in an energy scale, a careful calibration between the *flash-ADC* channels and the deposited energy was performed using three different γ -ray radionuclide sources (^{137}Cs , ^{88}Y and Am-Be).

Using a time-of-flight technique, the time to energy relation depends on the distance covered by neutrons from their production to the sample position. The effective neutron flight path of 184.21 m was determined by means of the well-known *s*-wave resonances of Au at low energy [9].

As said before, for the 2003 campaign the sample caused lots of problems. It was a powder sample of MgO encapsulated in an aluminium canning, which introduced uncertainties on the effective mass of magnesium and on the homogeneity of the sample areal density. The Al canning was by itself a source of background, and moreover the sample presented high impurities of $^{24,26}\text{Mg}$. For these reasons, in the 2012 campaign particular care was put in the choice of the new proper sample, and a self supporting metallic ^{25}Mg disc, isotopically enriched, was used. The characteristic of the sample are listed in table I. Part of the running time was dedicated to analyse a ^{197}Au sample for

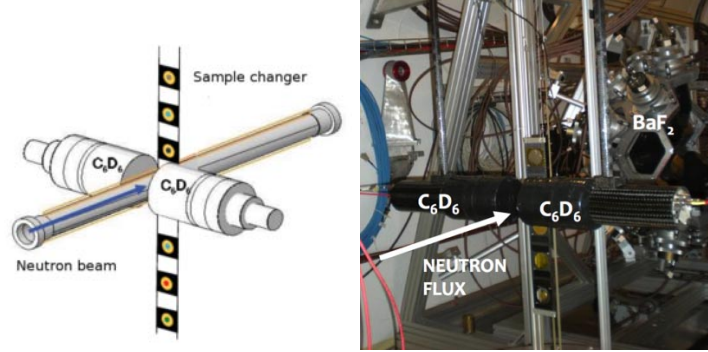


Fig. 2. – C_6D_6 detection system as a scheme for MC simulations and a picture of the n_TOF experimental area.

normalisation purposes, which will be discussed below. Moreover, to evaluate the energy dependence of the background, measurements were performed without any sample in beam.

2.2. Data reduction. – Capture events are recorded by means of the total energy detection technique, which requires that the detection efficiency to detect a capture event ε_c is independent from γ -ray spectrum multiplicity and from γ -ray energy distribution. More in details, it needs the proportionality between the detection efficiency and the total radiative energy released in a capture event:

$$(1) \quad \varepsilon_c = \sum \varepsilon_\gamma = k (B_n + E_n^{CM}),$$

where ε_γ is the efficiency to detect a single γ -ray, B_n is the binding energy and E_n^{CM} the incident neutron energy in the center-of-mass frame system. This proportionality is achieved by means of a low solid angle detection system, so that ε_γ is of the order of few percent, together with the Pulse Height Weighting Technique (PHWT) [10]. To calculate the weighting functions needed, the precise knowledge of the detector response as a function of energy is required, which is obtained from very detailed Monte Carlo simulations using Geant4 [11] with a complete description of the experimental setup.

The experimental quantity obtained with a time of flight technique is the experimental

TABLE I. – *Characteristic of the ^{25}Mg sample used for the capture experiment. The sample was borrowed from the Oak Ridge National Laboratory (ORNL), USA.*

Mass	Diameter	Thickness	Areal density	Isotopic composition
3.943 ± 0.002 g	20 mm	6.6 mm	3.03×10^{-2} at/barn	$^{25}\text{Mg} \sim 97.86\%$
				$^{24}\text{Mg} \sim 1.83\%$
				$^{26}\text{Mg} \sim 0.31\%$

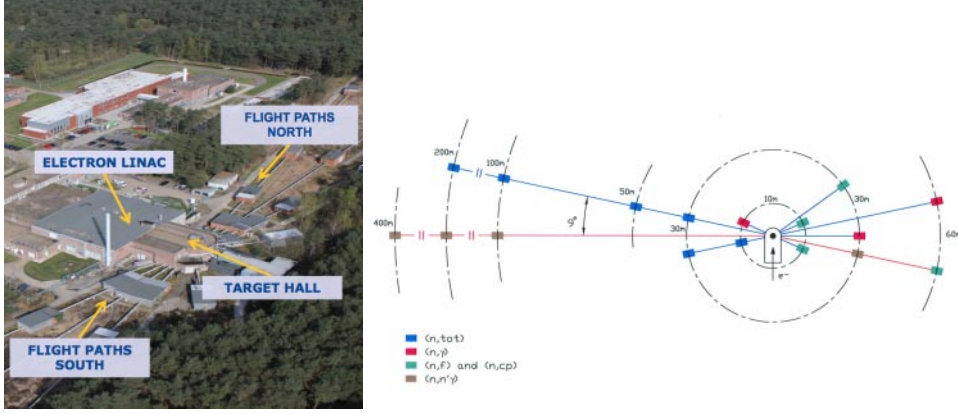


Fig. 3. – Top view and scheme of the GELINA facility.

yield. It could be expressed as a function of the incident neutron energy as

$$(2) \quad Y_c(E_n) = \frac{1}{f_b \varepsilon_c} \frac{C_w(E_n) - B_w(E_n)}{\phi_n(E_n)}.$$

Here, ε_c indicates the efficiency to detect a capture event and f_b the fraction of the neutron fluence ϕ_n intercepted by the sample, called beam interception factor. C_w is the weighted TOF-spectrum per proton pulse obtained with the ^{25}Mg sample and B_w the corresponding background contribution (obtained measuring without any sample in beam). Weighting functions are applied to both C_w and B_w spectra. The yields are calculated for both detectors separately and are afterwards combined for the determination of the final cross section.

Since the accurate determination of the beam interception factor and the detector efficiency is problematic, they were aggregated into one normalisation factor $N_c = 1/(f_b \varepsilon_c)$. This normalisation factor was obtained via the saturated resonance technique [12] by fitting the first saturated resonance at 4.096 eV of ^{197}Au using the R -matrix code SAMMY [13] and scaling the factor obtained for the neutron binding energy.

The neutron fluence $\phi_n(E_n)$ of the n-TOF facility has been accurately measured using five different detectors, in order to cover with the best precision obtainable all the energy range (more details can be found in refs. [5, 14]).

The experimental capture yield Y_c , the total cross section σ_{tot} and the capture cross section σ_γ are related by

$$(3) \quad Y_c(E_n) = (1 - e^{-n\sigma_{\text{tot}}}) \frac{\sigma_\gamma}{\sigma_{\text{tot}}},$$

where n is the areal density of the sample in atoms/barn. Therefore, measuring Y_c and σ_{tot} it is possible to extract σ_γ .

3. – Transmission experiment

3.1. Experimental method. – Total cross section on ^{25}Mg was performed at the GELINA time-of-flight facility of the Institute of Reference Materials and Measurements

TABLE II. – Characteristic of the ^{25}Mg sample used for transmission experiment. The sample was borrowed from the Oak Ridge National Laboratory (ORNL), USA.

Mass	Diameter	Thickness	Areal density	Isotopic composition
25.102 ± 0.002 g	36 mm	11.9 mm	5.95×10^{-2} at/barn	$^{25}\text{Mg} \sim 97.86\%$ $^{24}\text{Mg} \sim 1.83\%$ $^{26}\text{Mg} \sim 0.31\%$

(IRMM) in Geel, Belgium [8]. GELINA has been especially designed and built for high-resolution cross-section measurements. It is a multi-user facility, serving up to 12 different experiments simultaneously (see fig. 3), and providing a pulsed white neutron source, with a neutron energy range between 10 meV and 20 MeV. The GELINA facility consists of four main parts: a linear electron accelerator, a compression system, a neutron production target with a moderator and finally a series of neutron beam lines. Neutrons are produced via photonuclear (γ, n) and ($\gamma, 2n$) reactions and photofission (γ, f) reactions, which are induced by high-energy electron beam impinging on a mercury cooled rotating uranium target. To produce a white neutron spectrum from thermal energy up to few MeV, two water-filled beryllium moderators are placed above and below the uranium target.

The sample used, provided as well by the National Isotope Development Center of the ORNL - USA, is a metallic disc highly enriched in ^{25}Mg (it contains about 98% while the natural abundance is 10%). The characteristics are listed in table II.

The $^{25}\text{Mg}(n, \text{tot})$ measurement have been carried out at the 50 m measurement station, and the neutron beam is collimated to reduce its diameter to less than 35 mm at the sample position. The sample was placed in an automatic sample changer halfway through the beam line at a distance of about 23 m from the neutron source. In the experimental hall neutrons were detected by a Li-glass scintillator enriched to 95% in ^6Li and connected via a boron-free quartz window to a 127 mm EMI 9823 KQB photomultiplier (PMT) [15]. The design of the detector is shown in the left panel of fig. 4.

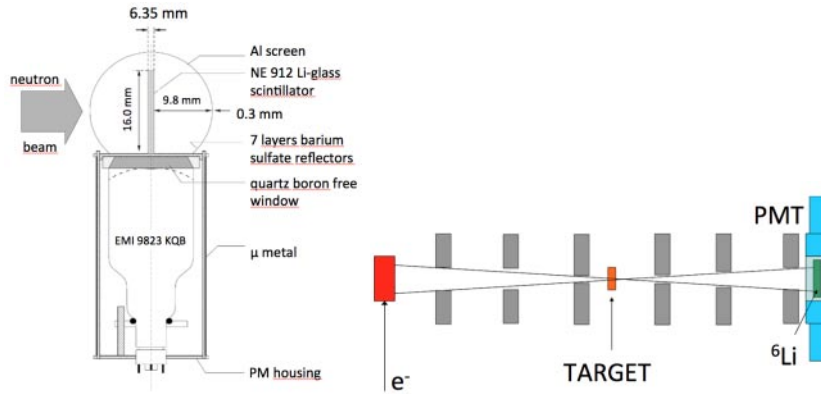


Fig. 4. – Design of the Li-glass scintillator and scheme of the experimental set-up for transmission measurements.

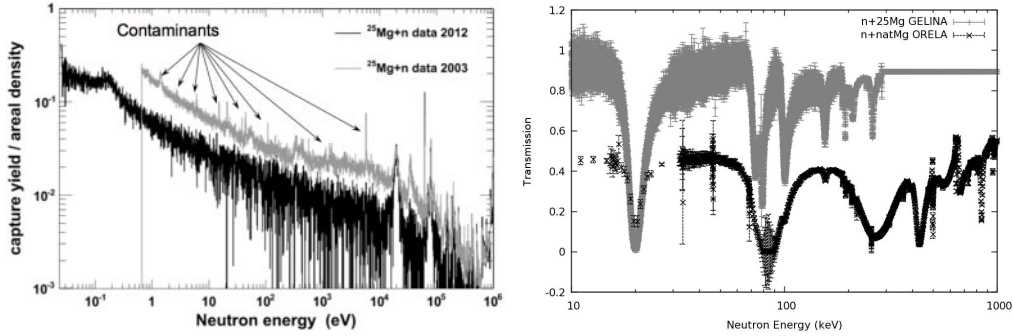


Fig. 5. – Capture yield and transmission coefficient for ^{25}Mg as function of the incident neutron energy. Left panel: comparison of the n_TOF capture data for the 2003 (grey) and 2012 (black) measurements. Right panel: transmission data on ^{25}Mg obtained at GELINA (grey) compared with a previous measurement on a $^{\text{nat}}\text{Mg}$ sample (black).

3.2. Data reduction. – The experimental observable in a transmission experiment is the transmission T , defined as the ratio between the number of neutrons detected in the experimental area (the neutron flux passing through the sample without interacting), and the neutron flux impinging on the sample:

$$(4) \quad T(E_n) = \frac{C_{\text{out}}(E_n)}{C_{\text{in}}(E_n)}.$$

This observable can be related, without considering the broadening effects, to the total cross section via its theoretical expectation value

$$(5) \quad T = e^{-n\sigma_{\text{tot}}}$$

under the proper experimental conditions of perpendicularity between the target and the incident neutron beam, and if all the neutrons that are detected have crossed the sample while neutrons scattered by the sample are ignored. As scheme of the experimental set-up is reported in the right panel of fig. 4.

4. – Preliminary results

Capture yield for ^{25}Mg has been obtained with C_6D_6 detectors in an energy range from thermal to hundreds of keV at the n_TOF facility. In the left panel of fig. 5 the comparison between the 2012 and the 2003 capture yield, properly normalised to the areal density of the samples, is shown. As it is clear from the figure, the new measurement is much more rid of contaminants than the previous one, with a better signal-to-background ratio, so that the resonance list could be cleaned up.

The transmission coefficient has been determined for the first time with an highly enriched sample of ^{25}Mg . In the right panel of fig. 5 the transmission data from this work are compared with the data present in the literature, which come from a previous measurement [16] where a natural Mg sample was used. It arises from the figure that the contribution of the others Mg isotopes, in particular of ^{24}Mg , is extremely high for the old measurement, and prevent to resolve the ^{25}Mg resonances. Using these new transmission

TABLE III. – MACS values for different astrophysical sites temperatures. Calculations made with resonance parameters extracted in this work are compared to the values obtained with the previous measurement [3] and the ones present in KADoNIS database [17].

Stellar site	Temperature (keV)	MACS (this work)	MACS (Massimi <i>et al.</i> [3])	MACS (KADoNIS [17])
He-AGB	8	3.9 ± 0.4 mb	4.9 ± 0.6 mb	4.9 mb
He-AGB	23	3.8 ± 0.4 mb	4.6 ± 0.6 mb	6.1 mb
He-AGB	30	3.5 ± 0.3 mb	4.1 ± 0.6 mb	6.4 ± 0.4 mb
He-Massive	25	3.7 ± 0.4 mb	4.4 ± 0.6 mb	6.2 mb
C-Massive	90	1.4 ± 0.1 mb	1.6 ± 0.2 mb	4.0 mb

data to obtain the total cross section will moreover improve a lot the precision of the capture cross section measurement and consequently the determination of spin-parities properties of ^{26}Mg states.

Both capture and transmission data are analysed with the R -matrix code SAMMY [13], obtaining the resonance energies as well as the partial width of resonances (Γ_γ and Γ_n). The fitting procedure used takes into account all the experimental effects which have an impact on the measurement: neutron multiple scattering in the sample, Doppler broadening and the experimental resolution of n-TOF facility [5]. A simultaneous resonance shape analysis of both capture and transmission data is performed, which leads to a much more precise result on resonance parameters with respect to the one obtainable analysing the two data sets separately. For instance, in fig. 6 the comparison between capture and transmission data in the 100 keV neutron energy range is shown. It is clear from the figure that the s-resonance at 100 keV is barely visible considering only capture data, due to its very large shape enlarged by the contribution of the multiple scattering, which prevents to distinguish it from the background. Combining transmission data, which are not affected by the multiple scattering, the parameters of this resonance, and so its contribution to capture cross section, could be estimated. By using the resonance parameters obtained as described above, the capture cross section was calculated and convoluted with a Maxwellian neutron energy distribution to derive the stellar cross section (MACS). The study of its uncertainty is ongoing. In a first approximation, it is dominated by its correlated part, attributable to PHWT, which includes normalisation, flux shape, beam interception factor and background subtraction.

In table III values of the MACS for different astrophysical sites temperatures are listed, comparing calculations with resonance parameters extracted in this work to the values present in KADoNIS database [17]. Values from this work strongly differs from both KADoNIS and 2003 ones, and in particular for most energies the MACS lays significantly below the others (see the left panel of fig. 7). This big difference observed will result in a further reduction of the poisoning effect in massive stars, which will modify the isotopic abundances of s process nucleosynthesis. In the right panel of fig. 7 this effect is shown for the Massimi *et al.* 2003 measurement [3]: the average enhancement in the heavy elements abundance is of about 30% with respect to the KADoNIS calculation. Moreover, this result will increase once inserting 2012 MACS values due to the further reduction of neutron poisoning effect.

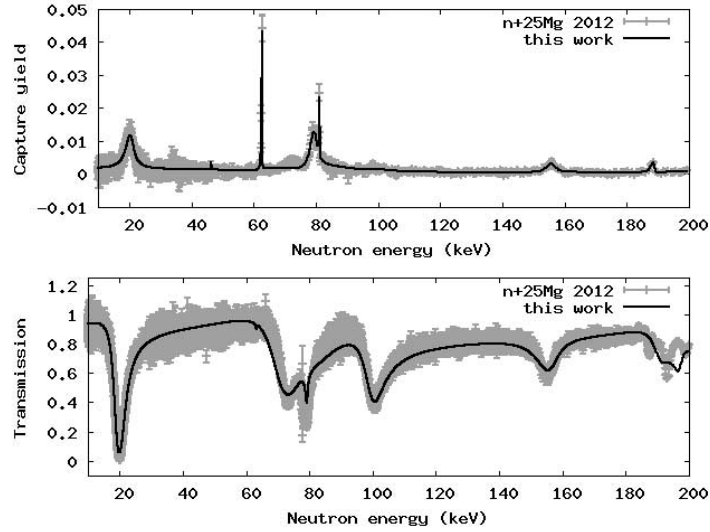


Fig. 6. – Comparison between capture (upper panel) and transmission (lower panel) data in the same energy range. Black lines are fits made with SAMMY code.

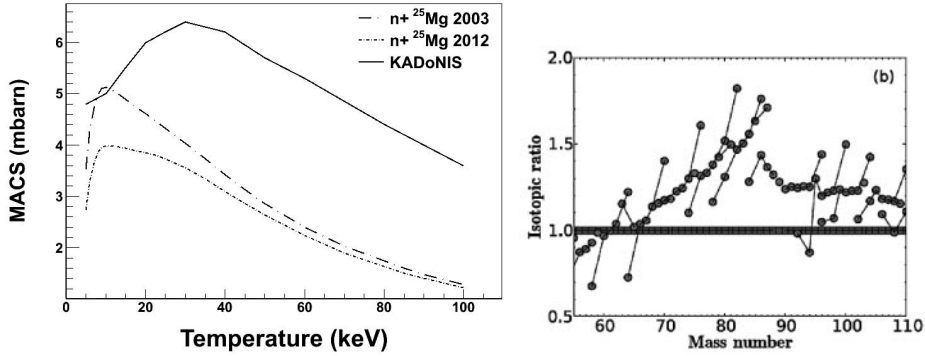


Fig. 7. – Left panel: stellar cross section as function of temperature calculated with resonance parameters from KADoNIS (solid line), Massimi *et al.* (dotted line) and this work (short dotted line). Right panel: ratio between the isotopic abundances calculated with the set of MACS values from KADoNIS database and with the MACS of ^{25}Mg by the 2003 campaign [3]. The average enhancement of 30% is due to the reduced neutron poisoning effect.

5. – Conclusions

The $^{25}\text{Mg}(n, \gamma)^{26}\text{Mg}$ reaction cross section has been measured at the n-TOF facility at CERN with an optimised experimental set-up, which allowed to obtain an extremely accurate and precise result. This reaction has a dual implication: first of all, its cross section, once averaged on a maxwellian distribution of neutron energies to obtain the effective stellar cross section (MACS), gives the poisoning effect of ^{25}Mg isotope for the onset of s process. Our results for the MACS are significantly lower than the values available in literature, which will result in a change of the isotopic abundances of the s process nucleosynthesis chain.

Secondly, the compound nucleus formed in the $^{25}\text{Mg} + n$ reaction, *i.e.* ^{26}Mg , is the same compound nucleus formed in $^{22}\text{Ne}(\alpha, n)^{25}\text{Mg}$ reaction. This is one of the two astrophysical neutron source for the s process, and its rate is still very uncertain mostly because of the poorly known properties of the states in ^{26}Mg . Therefore, a study of the spins and parities of ^{26}Mg levels populated with $^{25}\text{Mg}(n, \gamma)$ reaction is ongoing with the aim to extract important constraints for the reaction rate of the stellar neutron source.

To be as accurate as possible, a measurement of total cross section on ^{25}Mg was performed at the EC-JRC-IRMM facility GELINA in Belgium. Transmission data in literature were present only for ^{nat}Mg , which is dominated by ^{24}Mg . This new measurement, apart from sizeably improving the quality of total cross section data on ^{25}Mg , allows us to perform a more precise resonance shape analysis for capture cross section, and therefore to obtain a much more accurate and precise calculation of the effective stellar cross section.

To fully understand the role of ^{25}Mg isotope on stellar nucleosynthesis the measurement of the reaction $^{25}\text{Mg}(n, \alpha)^{22}\text{Ne}$ is under study. By means of the detailed balance procedure from this cross section we will be able to calculate the $^{22}\text{Ne}(\alpha, n)^{25}\text{Mg}$ one, which presents relevant inconsistencies in the low energy region. This challenging measurement will be performed at the n_TOF second experimental area (EAR-2), which is now under construction at CERN.

* * *

The author thanks the n_TOF Collaboration and the EC-JRC-IRMM Laboratory for the possibility given to perform capture and transmission measurements, and the INFN for financial support.

REFERENCES

- [1] BURBIDGE E. M., BURBIDGE G. R., FOWLER W. A. and HOYLE F., *Rev. Mod. Phys.*, **29** (1957) 547.
- [2] JAEGER M. *et al.*, *Phys. Rev. Lett.*, **87** (2001) 202501.
- [3] MASSIMI C. *et al.*, *Phys. Rev. C*, **85** (2012) 044615.
- [4] MASSIMI C. *et al.*, CERN-INTC-2012-003/INTC-P-320 (2012).
- [5] GUERRERO C. *et al.*, *Eur. Phys. J. A*, **48** (2013) 27.
- [6] MARRONE S. *et al.*, *Nucl. Instrum. Methods A*, **517** (2004) 389.
- [7] PLAG R. *et al.*, *Nucl. Instrum. Methods A*, **496** (2003) 425.
- [8] MONDELAERS W. and SCHILLEBEECKX P., *Not. Neutroni Luce Sincrotrone*, **11** (2009) 19.
- [9] MASSIMI C. *et al.*, *J. Kor. Phys. Soc.*, **59** (2011) 1689.
- [10] ABBONDANO U. *et al.*, *Nucl. Instrum. Methods A*, **521** (2004) 454.
- [11] AGOSTINELLI S. *et al.*, *Nucl. Instrum. Methods A*, **506** (2003) 250.
- [12] MACKLIN R. L. *et al.*, *Nucl. Instrum. Methods*, **164** (1979) 213.
- [13] LARSON N. M., Report N. ORNL/TM-9179/R7 (2008).
- [14] BARBAGALLO M. *et al.*, *Eur. Phys. J. A*, **49** (2013) 156.
- [15] SCHILLEBEECKX P. *et al.*, *Nucl. Data Sheets*, **113** (2012) 3054.
- [16] WEIGMANN H., MACKLIN R. L. and HARVEY J. A., *Phys. Rev. C*, **14** (1976) 1328.
- [17] DILLMANN I., PLAG R., KÄPPLER F. and RAUSHER T., in *EFNUDAT Fast Neutrons: Scientific Workshop on Neutron Measurements, Theory and Applications* (JRC-IRMM; Geel, 2009) <http://www.kadonis.org>.